Arabian Journal for Science and Engineering (2019) 44:6509–6523
https://doi.org/10.1007/s13369-019-03948-x

RESEARCH ARTICLE - EARTH SCIENCES

Structural Features of Kinwat Peninsular Gneissic Complex Along the Western Margin of Eastern Dharwar Craton, India

Ramakant Dinkar Kaplay[1] · Md. Babar[2] · Soumyajit Mukherjee[3] · Souradeep Mahato[3] · Sumeet Chavhan[2]

Received: 5 January 2018 / Accepted: 23 May 2019 / Published online: 29 May 2019

Abstract

The purpose of this study is to better understand the tectonics of the Deccan trap, India, for which we perform field studies and geomorphic analyses. The contact between the Eastern Dharwar Craton with the South East Deccan Volcanic province around Kinwat lineament (Maharashtra, India) is NW extension of the Kaddam fault. We study this contact in the present work. The region is predominantly NE-SW strike-slip faulted along with minor folds and boudins. These structures are confined to the granitic-gneissic basement. The faults reported in this study do not match with the earlier reported—E strike-slip faults, from Gokunda region near Kinwat city. The difference in the trend of faults indicates heterogeneity in the fault regime at local-scale. Different stress-axes at Gokunda and the study area led to the development of these two differently trending (NE-SW trending faults and—E strike-slip faults near Gokunda) fault regimes. Geomorphometric analyses connote that most of the study area is moderately tectonically active and tilted.

Keywords Deccan trap · Tectonics · Structural geology · Deformation

1 Introduction

The granitoids/gneissic basements of the Kinwat region belonging to Maharashtra state (India) belong to Peninsular Gneissic Complex where the contact between the Deccan trap and the Eastern Dharwar Craton exists (Fig. 1). Tectonics of Deccan trap has recently been worked out and reviewed by [1–8], etc. The Peninsular Gneissic Complex consists of complex gneisses, granitoids, and has played an important role in Precambrian crustal evolution [9–11]. The granitoids and gneisses in the study area are cut across by several quartzo-feldspathic veins, quartz veins and pegmatite veins. The region is also characterized by mafic intrusions and basic enclaves. The objective of the present research is to study and understand the structures in the area, as no detailed structural data were available. The study generated the primary data in regard with various structures for the first time, which were formerly not known and the study further revealed that the area is predominantly influenced by NE-SW strike-slip fault along with minor folds and boudins in eastern Dharwarian Cratonic area along the Kinwat lineament Kaplay et al. [3] of Kinwat area Nanded district of Maharashtra state, India.

✉ Soumyajit Mukherjee
smukherjee@iitb.ac.in

1 School of Earth Sciences, S.R.T.M. University, Nanded, Maharashtra 431 606, India

2 Department of Geology, DSM's Dnyanopasak College, Parbhani, Maharashtra 431 401, India

3 Department of Earth Sciences, Indian Institute of Technology Bombay, Powai, Mumbai, Maharashtra 400 076, India

2 Study Area

The region is bounded at South by the NW trending Kaddam fault lineament [12–14]. The NW extension of this lineament near Kinwat, referred to as the 'Kinwat lineament' [3], is important from structural point of view. The Kaddam fault lineament cuts through the Dharwar Craton rocks. The lineament is traceable also into the Deccan trap up to the Tapi Fault [14]. Sangode [14] further pointed out the possible active tectonic role of the Kaddam fault lineament as it intersects the seismically active zone of Purna fault towards NW and Bhadrachalam fault towards SE. Naganjaneyulu et al. [15] illustrated the Purna fault showing the deep crust beneath the Purna graben based on the Magnetotelluric data, while Bhadrachalam fault of Bhadrachalam seismic region is illustrated in the map [16]. Further, the evidence of deformations in the form of brittle to ductile deformations in the Precam-

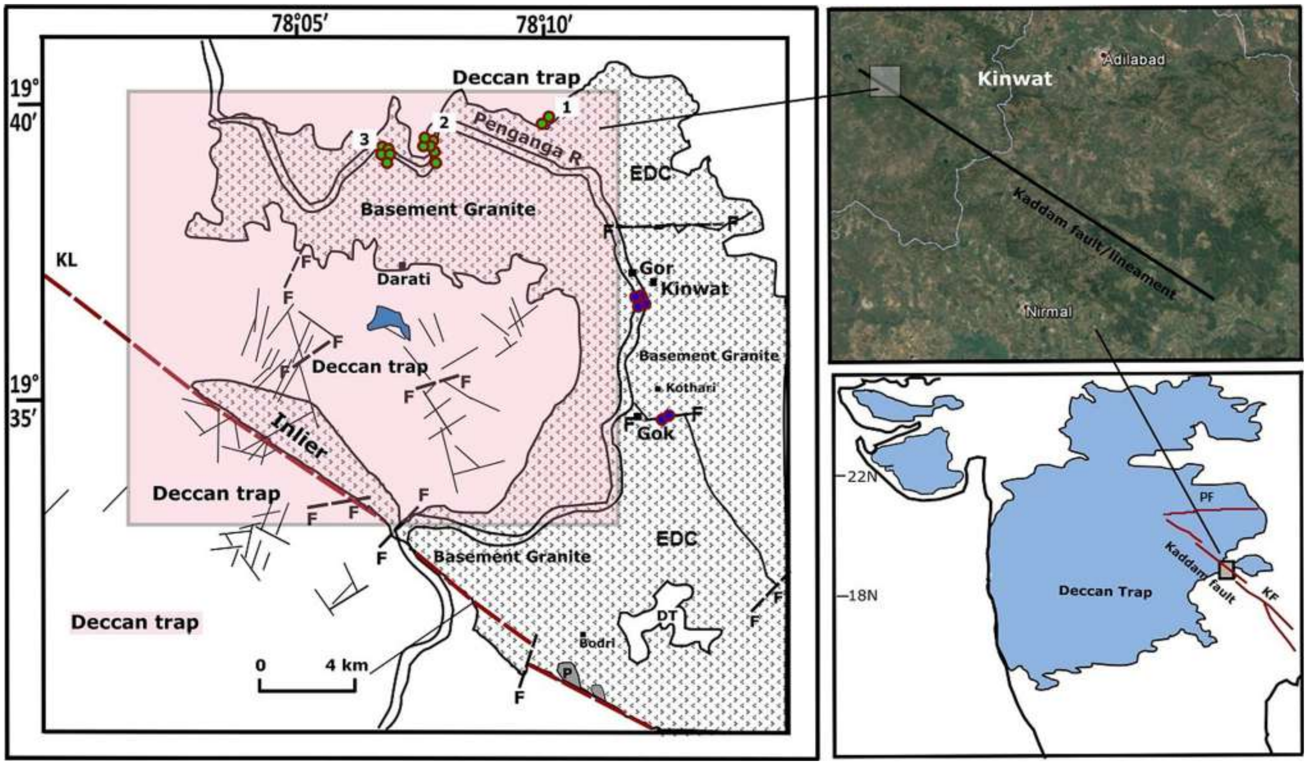

Fig. 1 Location map, after [41]. Green dots: deformations observed in this study at three different sites indicated by 1,2 and 3 towards north of the area. Black lines: NW-, EW- and NE-trending lineaments. Dash lines with F–F: faults; KL: Kinwat lineament, PF: Purna Fault, KF: Kaddam Fault (in lower inset figure), Gor: Gorakshan, Gok: Gokunda, Deccan trap: Plain area consist of Deccan volcanic province (DVP) and Basement Granite: Eastern Dharwarian craton (EDC) consisting of Peninsular gneissic complex marked as small dotted (filled) area. Inset eastern lower part is the area of DVP, and inset eastern upper part is the Google earth image of Kaddam lineament whose extension is in the form of Kinwat lineament occurring near Kinwat in Nanded district. River Penganga is the boundary between Nanded and Yeotmal District (Maharashtra state) with Nanded on northern and eastern parts of the river

brian terrain of Adilabad and Karimnagar in Andhra Pradesh [13] and recent reporting of strike-slip fault zone around Gokunda and parts of Kinwat, Nanded district, Maharashtra [3], confirms the tectonic role of the Kaddam fault lineament. We explored the region beyond Gokunda (towards SW, W and NW of Gokunda) to find out the structural features' of Peninsular Gneissic Complex. Structural features are observed towards NW at sites 1, 2 and 3 (Fig. 1).

3 Present Work

3.1 Geomorphic Characterization

We selected 27 sub-basins around the Kinwat lineament. The total area of these sub-basins is 402.03 km^2. The sub-basins were delineated from the SRTM DEM dataset, which is obtained from SRTM 1 Arc-Second Global DEM. The geomorphometric parameters include elongation ratio, asymmetric factor and hypsometric integral are determined to interpret the relation between tectonics and landforms as suggested by [17, 18]. We also studied pattern, density and frequency of drainage. Singh [19] pointed out that correlations can be easily done if the entire morphometric dataset is subdivided into different classes. Singh [19] also demonstrated that the zones are characterized by the relationship of the geomorphometric parameters on either side of the tectonic element ridge. Following [19, 20], we carried out spatial analysis to understand the relationship between sub-basins and tectonics.

3.2 Structures

EW strike-slip faulting is the most prominent deformation around Gorakshan and Kothari lineament [2, 3]. We selected several sites towards SW and W of Gokunda and few sites along the Penganga river ~ 11 km NW of Gorakshan to find out the extent of strike-slip fault zone. However, we noted structures at sites 1, 2 and 3 along the Penganga river only (Fig. 1). Fault-related slips/offsets are observed repeatedly at more than sixty spots. Many of these faults sub-parallel each other and display brittle and brittle-ductile deformations. The

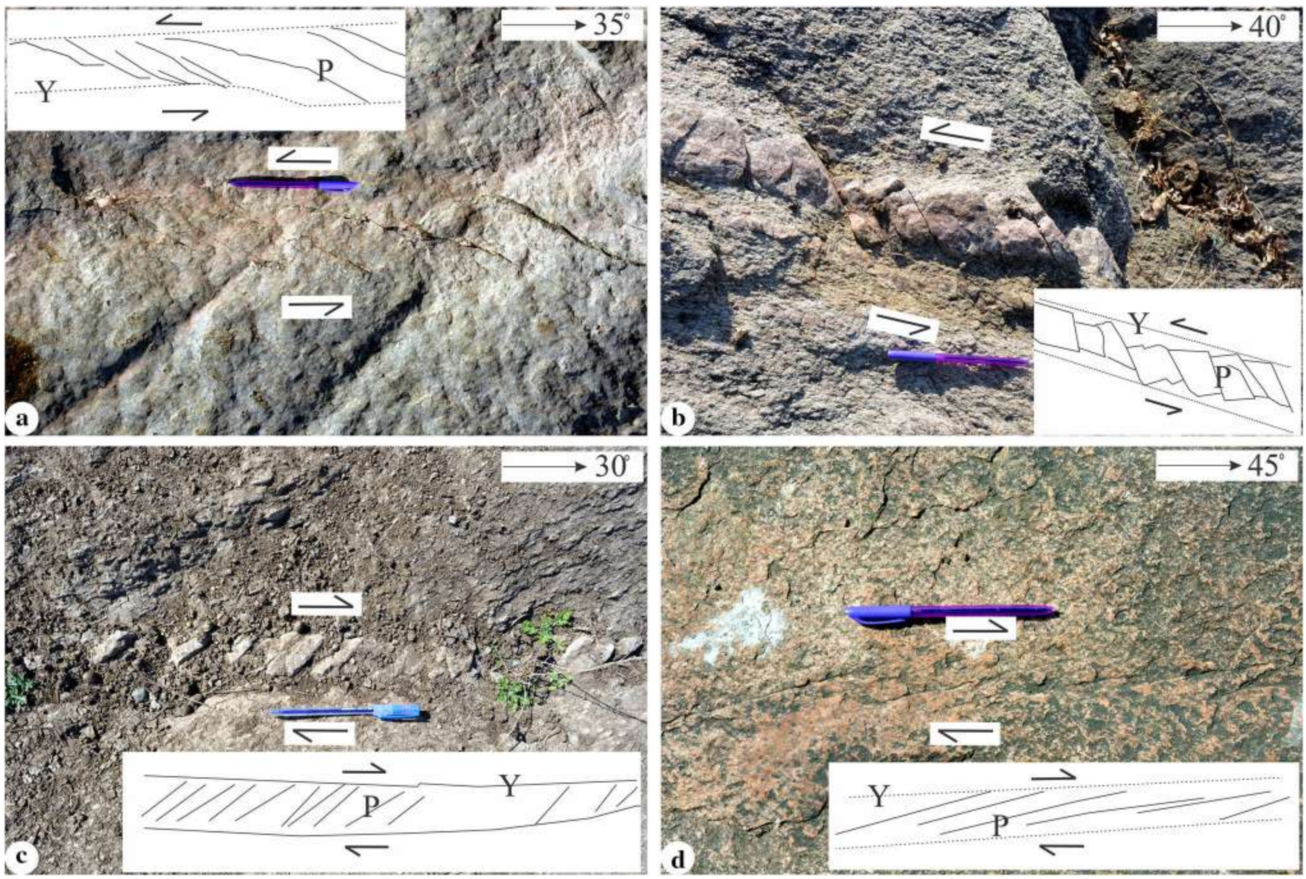

Fig. 2 In sub-horizontal sections. **a** Sinistral strike-slip fracture movement on granite gneiss. Y plane trends N35°E. **b** Sinistral strike-slipped/domino-glided quartzo-feldspathic vein. Individual slipped blocks are parallelogram-shaped, similar to parallelogram mineral fish [23]. Inter-block antithetic shear noted. Y plane trends N46°E. **c** Dextral strike-slipped quartzo-feldspathic vein. Y plane trends N30°E. **d** Dextral strike-slip by granite gneiss. Y plane trends N42°E. The numbers with arrows given in the small rectangles in the upper right corner of the figures are the indication of the compass direction of the study area in Penganga river bed near Kinwat Nanded district, Maharashtra, India

strike-slip faults (Fig. 2) are observed between locations 2 and 3 in ancient granitic rocks exposed on the riverbed at Kinwat in Nanded district (Fig. 1). The Y planes trend ~ NE. Both sinistral and dextral shear are found in this area (Fig. 2).

The felsic vein slips 4.0 cm along a N35°E striking fault (Figs. 3a,b). A quartz vein in granite slips 3.8 cm (Fig. 3c). We apply the commonly known shear sense criteria to find out the regional shear sense [21–37]. Some of the joints in the fault core terminate by curving towards another joint. Movement along fault is also accompanied by development of parallel joints in the wall rock. The joints in the wall rock have cut through the quartz vein. A gash joint terminates by curving towards a brittle plane (Fig. 3c). Figure 3d shows a pegmatite vein slipped at three places along sub-parallel fault planes. Here two sets of en-echelon joints develop in the wall rocks, which are mutually sub-parallel and ~ perpendicular to the fault planes ('C' in Fig. 3d). In Fig. 3e, f, mafic intrusions displace along thin felsic vein in a brittle manner. In all these cases, sharp displacement without any drag is noted, so they can be also called as n-type flanking structures [21, 29, 31, 34].

Small pegmatite veins in granites show breakage. The thin felsic vein acts as a fault plane (Fig. 4a). In Fig. 4b, a pegmatite vein is brittle slipped and in Fig. 4c, a felsic vein is brittle slipped. In another outcrop (Fig. 4d), one out of the two pegmatite veins (A) brittle slipped by other intersecting pegmatite vein (B). At F28, F29 and F30, both the veins are strike-slip faulted belonging presumably to a single generation of deformation.

The small pegmatite vein in one more outcrop is found to have strike-slip faulted at five places (Fig. 4e). Here, the two overlapping joints cutting across the pegmatite vein curve towards a perpendicular intersection with the other.

3.3 Brittle-ductile Deformation

Brittle-ductile deformations are also observed in the field. In one of the outcrops, the epidote vein slightly bends before

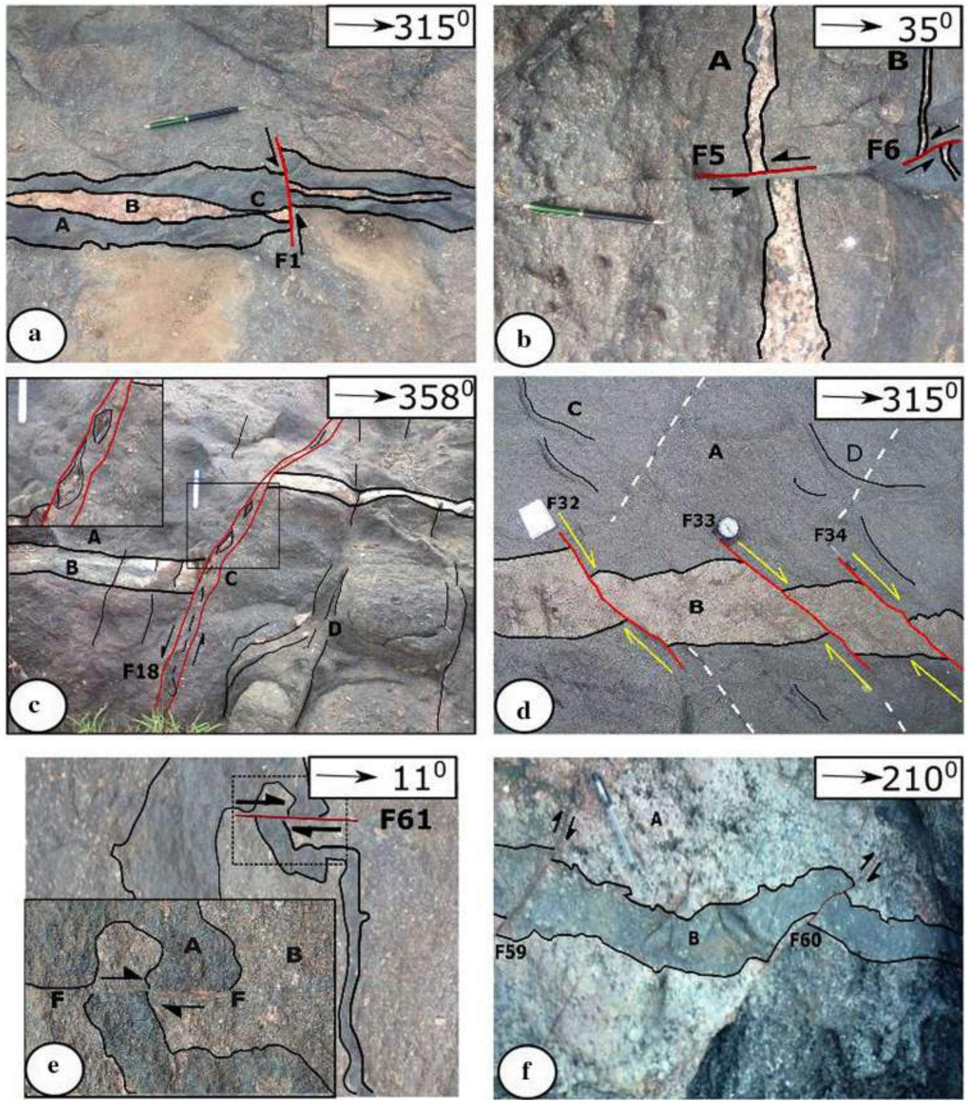

Fig. 3 **a** 'Intrusion in intrusion' in granitic rock. Felsic vein within mafic intrusion is brittle deformed. A: mafic intrusion, B: felsic intrusion, C: thinning of vein. The displacement is 4.0 cm. **b** Brittle deformed two pegmatite veins, and the displacement is 4.0 cm. **c** Brittle deformed quartz vein. A: granite, B: quartz vein, C: Fault core, D: gash joints; inset joints in fault core, the displacement is 3.8 cm. **d** Pegmatite vein (B) strike-slip faulted at two places. A: host rock, C: en-echelon joints parallel to fault lines, D: joints perpendicular to en-echelon joints. **e** Brittle slipped mafic intrusion. A: mafic intrusion, B: host rock. **f** mafic intrusion slipped at two places, A: host rock, B: mafic intrusion. These structures are observed at Site 3 in Fig. 1, lat. 19°38′8.665″N and long. 78°5′19.6197″E. F1, F5, F6, etc., are the fault numbers. The numbers with arrows given in the small rectangles in the upper right corner of the figures are the indication of the compass direction of the study area

breaking in a brittle manner (Fig. 5a) with the 14-cm strike-slip component. In other outcrop, felsic intrusion stretches before breakage (F39 and F40 in Fig. 5b). In Fig. 5c, the pegmatite vein drags along F17 before breaking in a brittle manner. At 'D' the vein thins. In Fig. 6, a folded quartz vein pinches at 'a' and 'e' besides its brittle deformation. At 'b', 'c' and 'd', the vein drags and deforms in a ductile–brittle manner, while at 'd' brittle deformation is noted. A pull-apart structure (Fig. 7) is noted at a single location. Here, the vein is ~ 2.1 cm pulled apart. Such structures form usually in the release area between sub-parallel faults [38].

3.4 Ductile Deformation

In Fig. 8a, two parallel basic intrusions slip sinistrally inside a thin shear zone in a ductile manner. The sheared part of the vein is thickened. Foliations did not develop inside the shear zone. In Fig. 8b, the felsic vein is ductile deformed at F35 (Fig. 5d), at F34 (Fig. 3d) and F37 (Fig. 6d). A quartzo-feldspathic vein is chevron folded (Fig. 8b). The axial surfaces orient N30ºW-S30ºE indicating compression along N60ºE-S60ºW.

The granitic-gneissic rock is well foliated (Fig. 9a). The foliation planes are sub-vertical and trends ~ N. The gneissic rock consists of mafic rocks as boudinaged enclaves (Figs. 9a, b, 10a). The extension direction represented by boudins nearly parallels foliation planes within the granite gneiss. At location 3, a 100 m * 20 m zone (Fig. 9) show 160° trending foliations and boudins (Fig. 10). Few boudins (Fig. 10c) display eye-shaped symmetric geometry (as reviewed in [31], which are not clear-cut shear sense indicator. S- and C-planes indicating ductile shear is also observed (Fig. 10d) in this zone. The ductile shear sense is defined by sigmoid dense foliation planes and connotes a dextral shear along N45°E trending C-planes (Fig. 11). In Fig. 12a, small quartz vein in mafic intrusion is found to

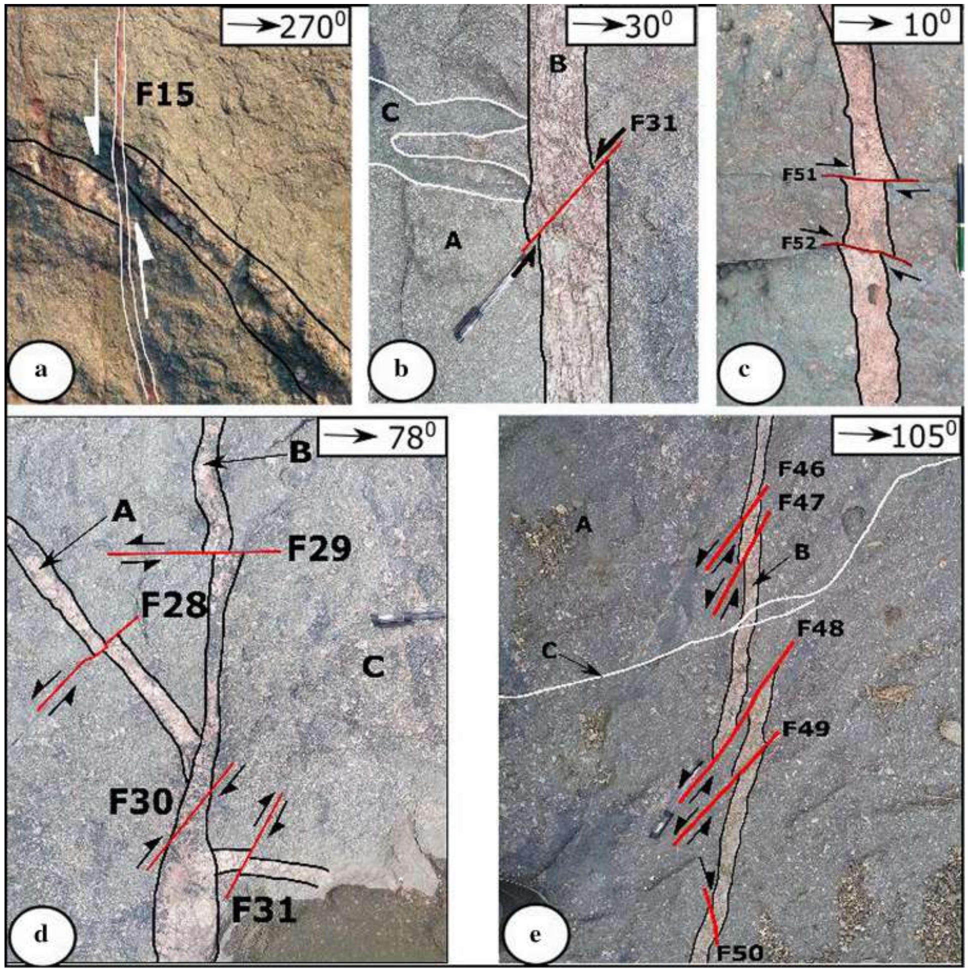

Fig. 4 **a** Pegmatite vein brittle slipped along a thinner felsic vein in host granite rock. **b** Pegmatite vein strike-slip faulted; A—host rock granite, B—pegmatite vein and C—mafic enclave. **c** Felsic vein brittle slipped at two places at faults F51 & F52 host rock granite. **d** A pegmatite vein (A) brittle slipped along another pegmatite vein (B). Both the veins are further brittle faulted at F28, F29 and F30. **e** Felsic vein faulted at five places (faults from F46 to F50). A: host rock granitic gneisses, B: felsic vein and C: joint cutting across felsic vein. These features are observed at Site 3 (Fig. 1), lat. 19°38′7.9028″N and long. 78°5′19.812″E. The numbers with arrows given in the small rectangles in the upper right corner of the figures are the indication of the compass direction of the study area

be showing boudinaged structure. In another outcrop, a pegmatite vein is also boudinaged (Fig. 12b). In Fig. 12c, the boudinaged felsic vein is further brittle deformed.

Table 1 presents the detail of trends and slip senses of the faults. The region is predominantly strike-slip faulted, with 28 sinistral and 35 dextral cases. Dissimilar net slips are observed in one case (Fig. 3b). Here, the offset at F5 is 6 cm and at F6 is 3.5 cm. As expected, net slip may vary along the length of the same fault [40].

Figure 13 presents fault trends: dominantly N70°–90°E. This matches with the Gorakshan and the Kothari lineaments in the adjoining region [3]. The other prominent trend ranges N70°–90°W. NW–SE strike-slip faults also corroborate with the main Kinwat lineament. Interestingly, the slip along NW–SE trending faults exceeds that of the NE-SW fault.

3.5 Lineament

The Kinwat lineament, a NW extension of the Kaddam fault/lineament, is exposed geomorphologically as a valley (3D model/presentation: Fig. 14). The valley is up to 30 m deep, and it shallows gradually towards NW. The side of this valley, particularly near the Kinwat inlier, is quite steep (Fig. 14) and is vegetation-covered. Several structurally controlled river paths close to this lineament can be observed in (Google Earth) remote sensing images.

The Kinwat inlier is exposed towards the northern side of this lineament. It shows sharp contact with the younger basalt towards the southern side of the lineament (Fig. 1). The lineament continues into the Deccan trap towards NW. Continuity of Kaddam fault/lineament within the Deccan volcanic province could imply its Tertiary reactivation [14].

4 Geomorphic Indicators of Tectonics

Geomorphic indices indicate relationship between basin morphology and tectonics [17, 18]. We selected 27 sub-basins, located within the two districts Yeotmal and Nanded in the Maharashtra state, aiming this. Interestingly, strike-slip faults are reported recently from the Gorakshan region near Kinwat [3].

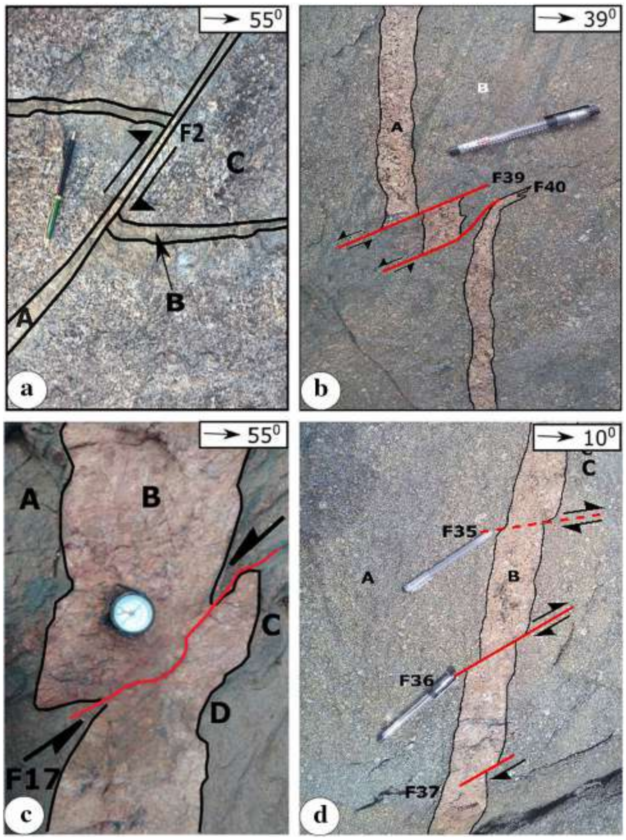

Fig. 5 **a** Epidote vein (B) displaced in a brittle-ductile manner along a felsic vein (A); C: host rock granite. **b** Felsic vein deformed in a brittle-ductile manner at two places; at F39 and F40, at F40 the drag is more compared to F39. **c** Pegmatite vein (B) in granitic host rock (A) shows brittle-ductile deformation at 'C'. At 'D' the vein thins. **d** Felsic vein ductile deformed at F34, F35 and F37. These features are observed at Site 3 (Fig. 1), lat. 19°38′9.1927″N and long. 78°5′19.8296″E

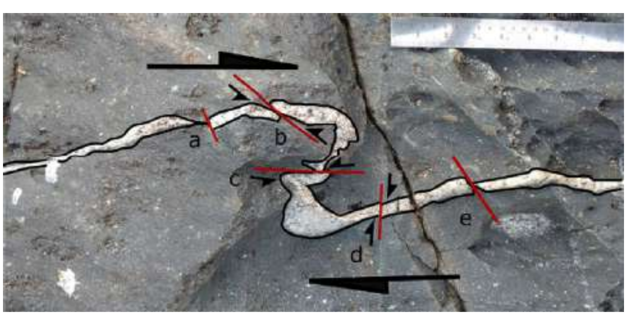

Fig. 6 A folded quartz vein showing pinching structure at 'a' and 'e' and ductile–brittle deformation at 'b', 'c' and 'd'. F54 to F58 are deformations developed at respective places from a to e

Fig. 7 Pulled apart structure shown by felsic vein, the displacement is 2.1 cm in felsic vain

Dendritic drainage characterizes most of the sub-basins. However, the drainage pattern along the Kinwat lineament passing through sub-basins 1–3 shows trellis pattern, which could indicate (blind) fault (Fig. 15a, b). Dendritic drainage pattern in different sub-basins shows varying number of streams. In sub-basins 11 and 15 (Fig. 16a, b) a minimum 11 number of streams developed. On the other hand, a much greater number of streams developed in sub-basins 2 (Fig. 16c) and 4 (Fig. 16d), 538 and 712, respectively.

A basin elongation ratio < 0.5 indicates that it is tectonically active. Values ranging 0.5–0.75 reflect slight/moderate tectonic activity, whereas > 0.75 denote inactive basins [39]. The sub-basins from the study area have either moderate (sub-basins 1–11, 13–17, 19, 21–26) or high elongation ratio (sub-basins 12, 18, 20, 27). Figure 17a classifies these sub-basins.

As per [41], an asymmetry factor (AF) ~ 50 indicates that the stream network flows over a stable region. Unstable tectonic setting would indicate AF < 50 or > 50 [18]. Here we consider an AF ranging 45–55 as near normal indicative of tectonic stability, and > 55 or < 45 connoting tectonically tilted sub-basins. The sub-basins 3, 5, 8, 11, 16 and 19 possess AF of 45–55. The AF values of the sub-basin numbers 1, 2, 14, 18, 20, 22, 24 exceed 55 and sub-basin numbers 4, 6, 7, 9, 10, 12, 13, 15, 17, 21, 23, 25, 26, 27 are lower than 45 (Fig. 17b). Most of the sub-basins in the study area are tectonically active. Though less numerous, the inac-

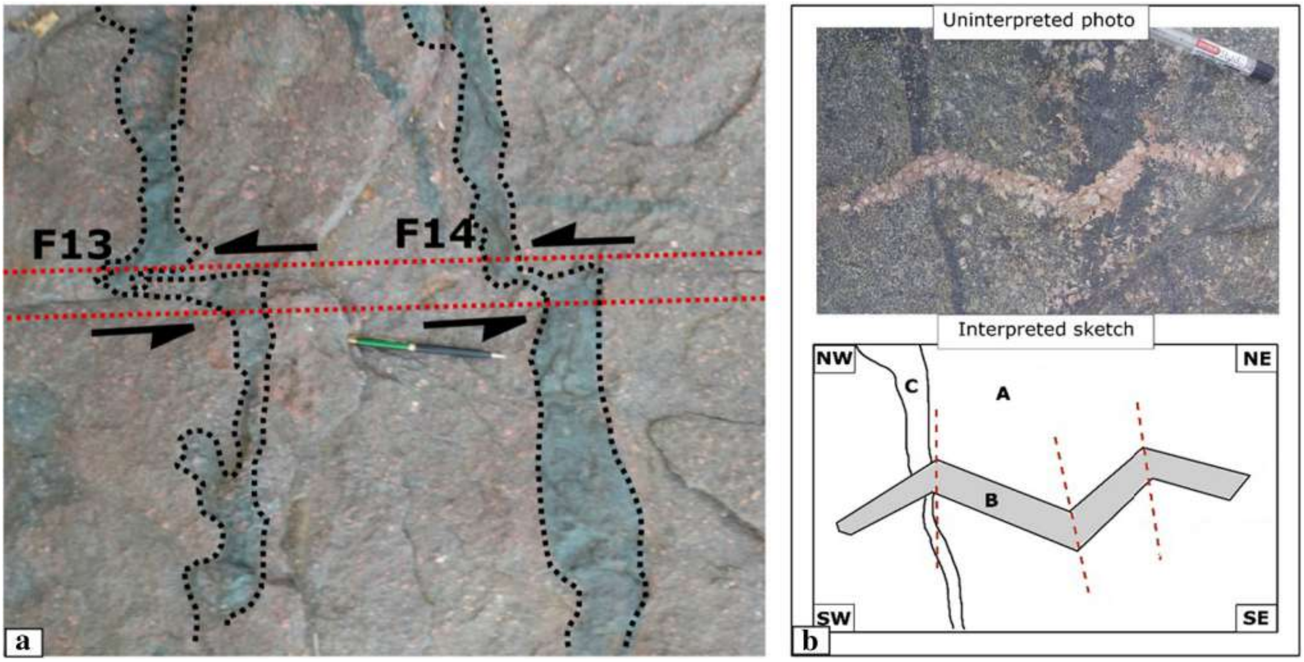

Fig. 8 **a** Two parallel basic intrusions are displaced in a ductile manner, F13 and F14 are the deformations observed in the area. Red dots indicate the zone of deformation with black arrows indicating the direction of deformation. **b** Quartzo-feldspathic vein shows chevron folding observed in both un-interpreted photograph and the interpreted sketch of the area. 'A' host rock, 'B' quartzo-feldspathic vain showing ductile deformation and 'C' mafic intrusion along hinge area of fold

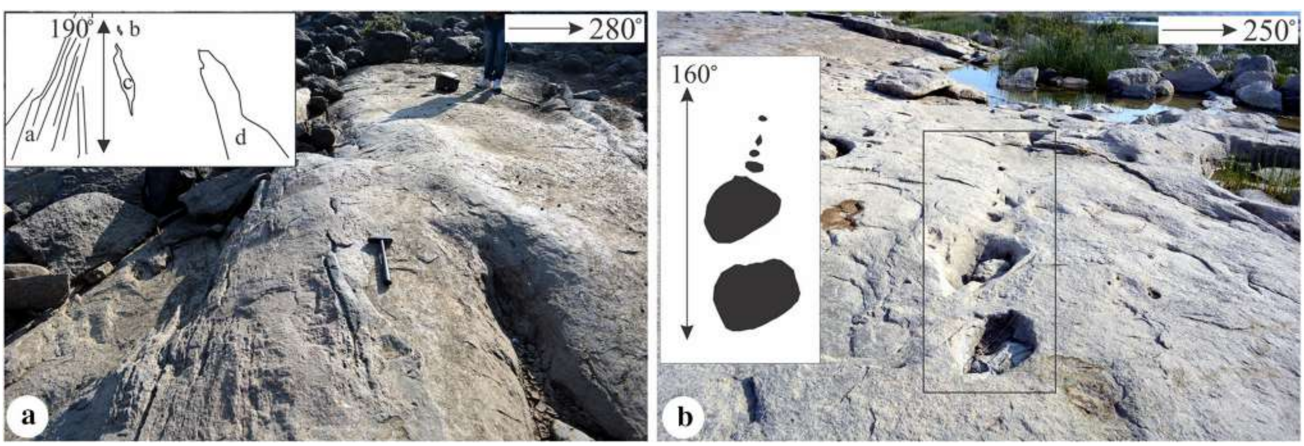

Fig. 9 Field photograph of granite gneiss exposed on the river bed. The river trends ~ N20°E. **a** Sub-vertical foliations trend ~ 190° marked as 'a'. Boudinaged mafic enclaves (marked as 'b–d') follow ~ N–S foliation trend. White-coloured rectangular area in the figure is the sketch of the photograph for detail illustration of foliation and boudinage. **b** Boudins: extension direction trends 160°–340°. White-coloured rectangular area in the figure is the sketch of the photograph for detail illustration of boudinage extension. The rectangular area in the middle part of the **b** is to illustrate which area is drawn in the rectangular sketch. Numbers in the figures means the direction of compass direction of the area or the feature

tive sub-basins locate randomly. The drainage anomalies are mostly associated with WNW-ESE direction as well as the NW–SE lineament zone for about 2–3 km. Asymmetry factor (AF) detects tectonic tilt in basins [41]. The geomorphologic parameters estimated here suggest slight or moderate tectonic tilt of the area. However, anomalous AF along WNW-ESE and NW–SE may be due to the adjustment of a probable NW–SE lineament.

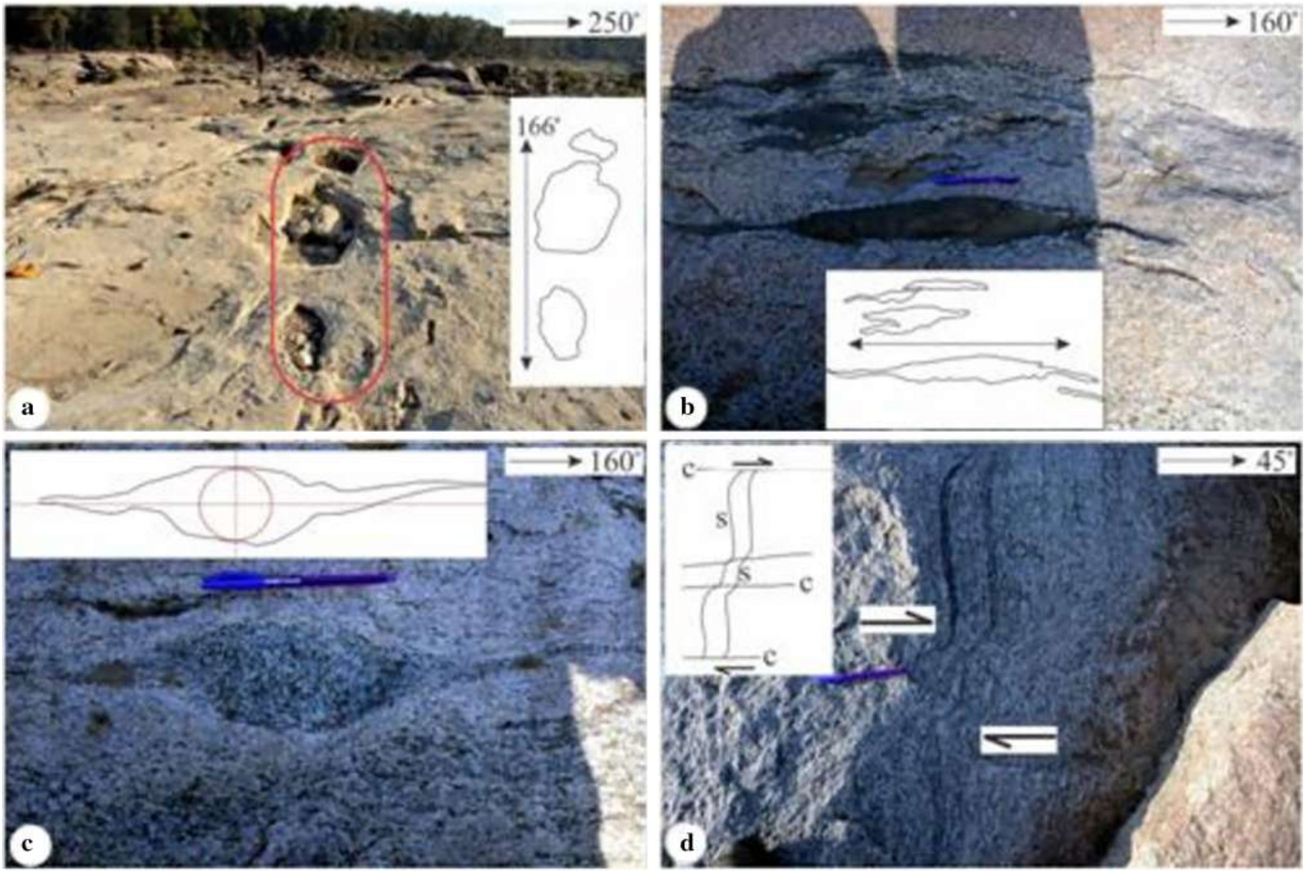

Fig. 10 Field photograph of boudins in horizontal section: **a** extension direction being 166°. **b**, **c** Boudinaged mafic enclaves with extension direction: 160°. **d** Well-developed S- and C-planes within granite gneiss. C-planes trend ~ N45°E. White-coloured rectangular areas in the figure are the sketches of the photographs for detail illustration of boudinage extension, S and C plains

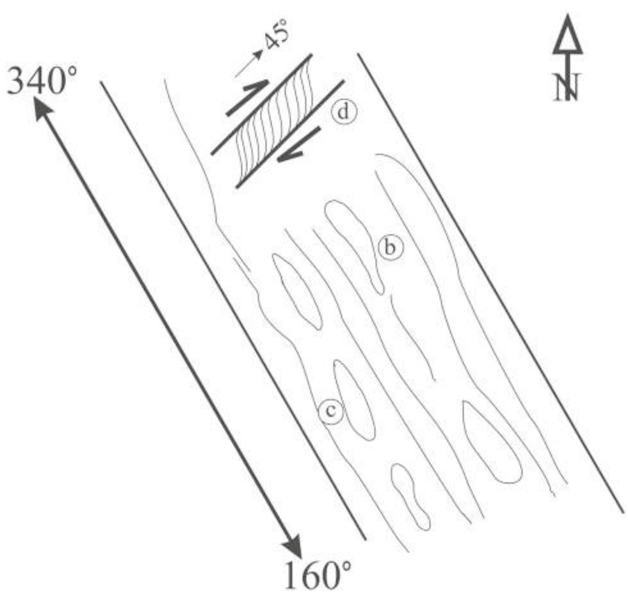

Fig. 11 A schematic sub-horizontal exposure shows the position of the features in Figs. 10b–d. The zone trends 160°–340°. At position 'd', S- and C-fabric is well developed. C plane trends N45°E. 'b', 'c' and 'd' in circle indicate the line diagram of actual photographs of the structures shown as 'b', 'c' and 'd'

5 Discussions & Conclusions

The Indian craton is cut across by several continental-scale shear zones. The craton is also characterized by extreme sheared rocks that intrusives cut across. Cratonic part exposed near Kinwat in the study area is similarly criss-crossed by shear zones, and felsic and basic intrusives.

Strike-slip faults in Kinwat region are well documented because of good exposures particularly along the Penganga river. These intracratonic small-scale faults localize within the granitic rocks, which indicate their antiquity.

Zones of strike-slip faults usually consist of (sub) parallel faults [38]. These strike-slip faults are characterized by *(i)* pinnate or en-echelon arrangement, *(ii)* sense of slip: dextral (0.5–38 cm slip) or sinistral (0.2–38 cm slip); and *(iii)* smaller faults occurring inside larger fault zones [38].

Most of the faults appear as hairline cracks/joints (Fig. 3d). In few cases, however, up to 5-cm-thick fault core is observed (Fig. 3c). [42] pointed out that the deformation on varying scale is observed in the damage zone surrounding the fault

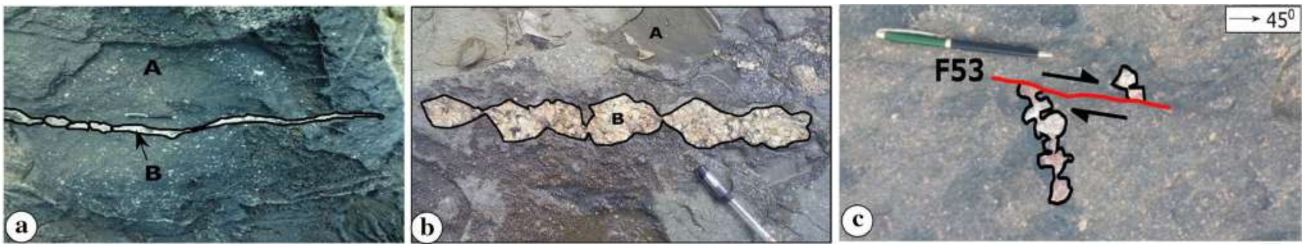

Fig. 12 **a** Quartz vein (B) within basic intrusion (A) shoe development of boudinaged. **b** Felsic vein (B) shows boudinage structure in host rock granitic gneiss (A). **c** Felsic vein, showing boudinage structure, is deformed in a brittle manner. The red line is the line of deformation, and F53 is the number of fault line. The number with arrow given in the small rectangle in the upper right corner of the figure is the indication of the compass direction of the study area

Table 1 Trends and shear senses of slip faults found in this study from Darati (see Fig. 1 for location 3)

Sl. no.	Structure no.	Deformation regime (B: Brittle, D: ductile, BD: brittle ductile	Type of fault	Shear sense	Strike	Net slip (cm)
1	F_1	BD	Strike slip	Sinistral	N35°E	4.5/4.0
2	F_2	BD	Strike slip	Dextral	NS	14
3	F_3	B	Strike slip	Dextral	N30°E	18
4	F_4	B	Strike slip	Sinistral	N80°W	38
5	F_5	B	Strike slip	Sinistral	N35°E	6
6	F_6	B	Strike slip	Sinistral	N28°E	3.5
7	F_7	B	Strike slip	Sinistral	N20°E	7.4
8	F_8	B	Strike slip	Dextral	N40°E	1
9	F_9	B	Strike slip	Sinistral	N39°E	1.2
10	F_{10}	B	Strike-Slip	Dextral	N25°E	1.4
11	F_{11}	B	Strike slip	Dextral	N30°E	2
12	F_{12}	B	Strike slip	Dextral	N46°E	0.3
13	F_{13}	D	Strike slip	Sinistral	N45°E	11.5
14	F_{14}	D	Strike slip	Sinistral	N45°E	3
15	F_{15}	B	Strike slip	Sinistral	NS	10
16	F_{16}	B	Strike slip	Sinistral	N40°E	2
17	F_{17}	BD	Strike slip	Sinistral	N15°E	16
18	F_{18}	B	Strike slip	Sinistral	N80°W	38
19	F_{19}	B	Strike slip	Dextral	N10°E	2
20	F_{20}	B	Strike slip	Dextral	N28°E	3.6
21	F_{21}	B	Strike slip	Dextral	N48°E	1
22	F_{22}	B	Strike slip	Dextral	N35°E	2.4
23	F_{23}	B	Strike slip	Dextral	N25°E	2
24	F_{24}	B	Strike slip	Sinistral	N35°E	1.4
25	F_{25}	B	Strike-Slip	Sinistral	N45°E	1.5
26	F_{26}	B	Strike-Slip	Dextral	N35°E	0.7
27	F_{27}	B	Strike slip	Dextral	N35°E	1.3
28	F_{28}	B	Strike slip	Sinistral	N43°E	2
29	F_{29}	B	Strike slip	Sinistral	N78°E	1.4
30	F_{30}	B	Strike slip	Dextral	N18°E	1.5
31	F_{31}	B	Strike slip	Sinistral	N17°W	2
32	F_{32}	B	Strike slip	Dextral	N01°W	11
33	F_{33}	B	Strike slip	Dextral	N20°W	16.5

Table 1 continued

Sl. no.	Structure no.	Deformation regime (B: Brittle, D: ductile, BD: brittle ductile	Type of fault	Shear sense	Strike	Net slip (cm)
34	F_{34}	B	Strike slip	Dextral	N17°W	20
35	F_{35}	D	Strike slip	Dextral	N20°E	3
36	F_{36}	B	Strike slip	Dextral	N20°W	2.5
37	F_{37}	B	Strike slip	Dextral	N20°W	1.8
38	F_{38}	B	Strike slip	Dextral	N25°E	2.7
39	F_{39}	B	Strike slip	Sinistral	N15°E	4.5
40	F_{40}	D	Strike slip	Sinistral	N15°E	5.5
41	F_{41}	B	Strike slip	Dextral	N05°E	1.5
42	F_{42}	B	Strike slip	Dextral	N20°E	3.5
43	F_{43}	B	Strike slip	Dextral	N20°W	3
44	F_{44}	B	Strike slip	Dextral	N85°W	1
45	F_{45}	B	Strike slip	Sinistral	N25°E	1.3
46	F_{46}	B	Strike slip	Sinistral	N51°E	0.5
47	F_{47}	B	Strike slip	Sinistral	N45°E	1
48	F_{48}	B	Strike slip	Sinistral	N50°E	11.3
49	F_{49}	B	Strike slip	Sinistral	N62°E	1
50	F_{50}	B	Strike slip	Dextral	N09°W	0.5
51	F_{51}	B	Strike slip	Dextral	N10°E	1.6
52	F_{52}	B	Strike slip	Dextral	N40°E	1.7
53	F_{53}	B	Strike slip	Dextral	N53°E	8.2
54	F_{54}	D	Strike slip	Dextral	N20°W	–
55	F_{55}	B	Strike slip	Sinistral	N40°W	0.5
56	F_{56}	BD	Strike slip	Sinistral	N80°W	1.0
57	F_{57}	B	Strike slip	Dextral	N05°E	0.2
58	F_{58}	BD	Strike slip	Dextral	N10°W	–
59	F_{59}	B	Strike slip	Dextral	N20°W	2.0
60	F_{60}	B	Strike slip	Dextral	N10°W	1.9
61	F_{61}	B	Strike slip	Dextral	N10°E	5.0

B brittle, *BD* brittle ductile, *D* ductile

core. In the study area, however, most of the small-scale faults are not associated with the damage zone.

These newly reported strike-slip faults do not resemble in trend with those around Gokunda region reported earlier by Kaplay et al. [3]. We, in this study, report few more evidence of strike-slip faults; however, these faults do not match with the earlier reported ~ E strike-slip faults, from Golunda region near Kinwat city, as most of them trend either NE or NW. However, they may belong to the same master fault system, extended towards NW, which runs parallel close to the Kinwat lineament.

Based on values of elongation ratio of the sub-basins (Fig. 17a), it is concluded that except sub-basins 12, 18, 20 and 27, all other sub-basins in the study area are slight to moderately tectonically active. Faulting is reported from site 2, which is just at the mouth of tectonically inactive sub-basin 18. The reason for such inactivity needs further study.

Asymmetric factor indicates that except sub-basins 3, 5, 8, 11, 16, 19 all other sub-basins are slight to moderately tectonically tilted (Fig. 17b).

The study area is dissimilar in terms of both lithology and geological structures when compared to its southern portion. The NW extension of Kaddam fault/lineament, referred to as 'Kinwat lineament' [2, 3], is present as a trench (Fig. 12). Basalts are present at the southern side, while granite gneisses (in the form of inlier and basement) exist at the northern side of the Kinwat lineament. Singh [19] divided the basins across the tectonic element (ridge) to find out whether the morphometric parameters across the ridge show some typical feature. In our study area, we divided the four sub-basins: 1–4, which are cut by the Kinwat lineament into two zones: a northern side and a southern side. Parts 'a', 'c', 'e' and 'g' are at the northern side, while 'b', 'd', 'f' and 'h' at the southern side of the Kinwat lineament (Fig. 18a, b). This is done to

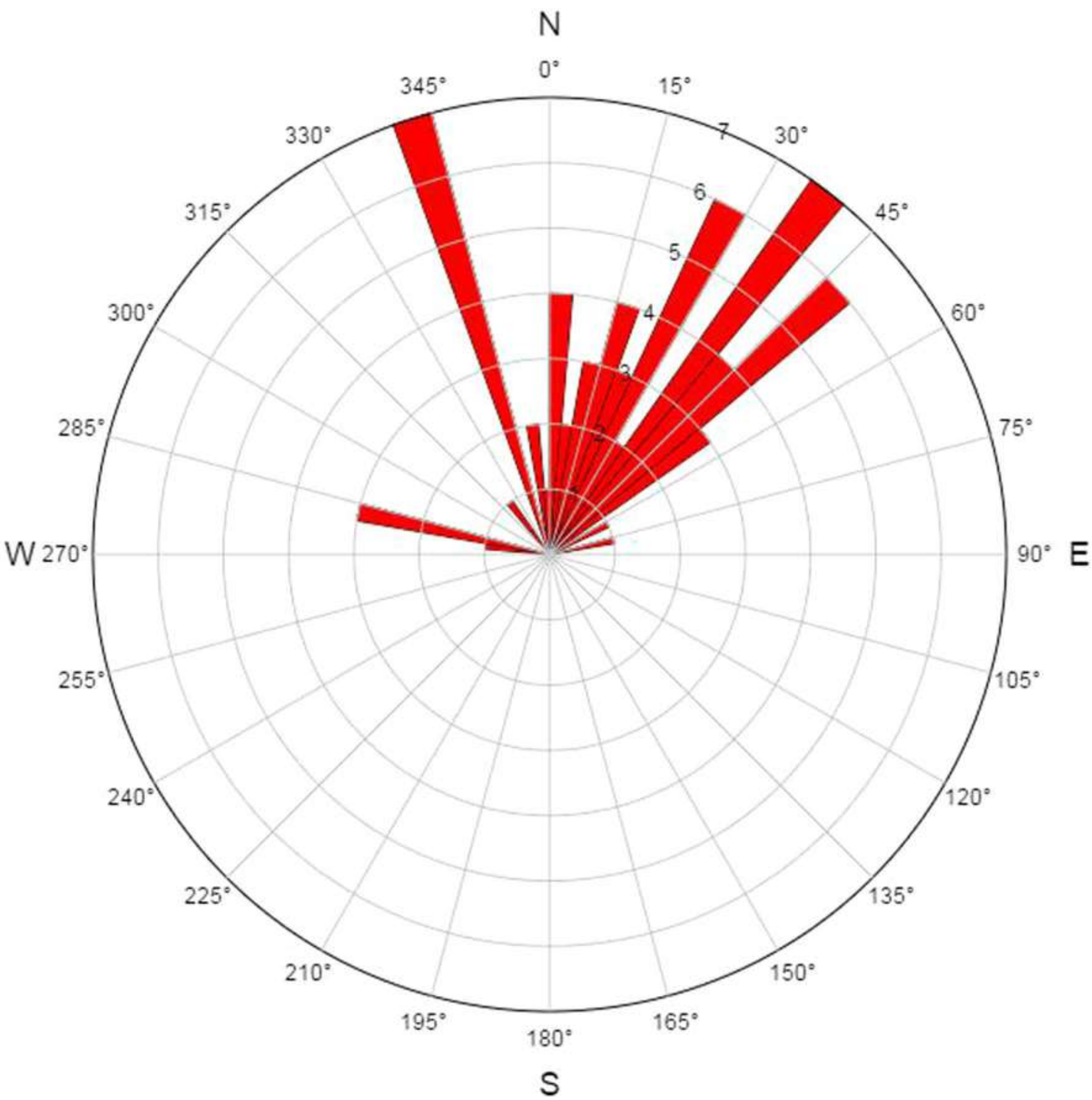

Fig. 13 Rose diagram shows the trends of strike-slip faults from the studied sections

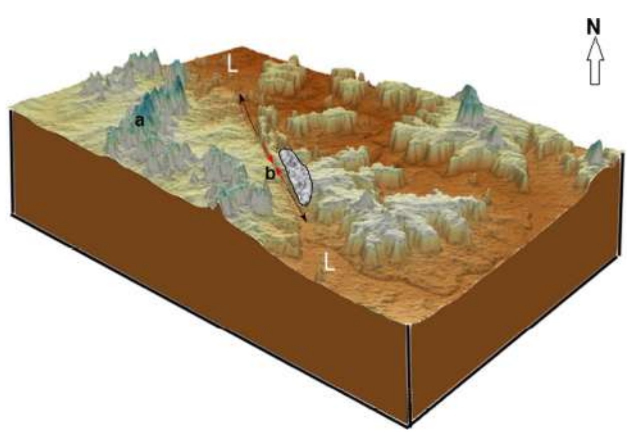

Fig. 14 Kinwat lineament exposed in the form of (**a**) hilly terrain in the bordered area of the basin and (**b**) deep valley in the centre. Black and red arrows in the centre indicate the directions of streams flowing along the lineament (L–L shown as white letters)

investigate if geomorphometric parameters across the Kinwat lineament show any typical characteristic features. We found that stream frequency and drainage density across the lineament vary (Fig. 18a, b). Drainage density and frequency north to Kinwat Lineament is different from those towards south. This can be attributed to different rocks across the lineament. Towards North of Kinwat lineament in sub-basin 2, ancient granite is exposed, while towards its south occurs basalt.

Morphometric analysis of the study area reveals:

i. Most of the study area (80%) is moderately tectonically active as the elongation ratio of most of the sub-basins is moderate.

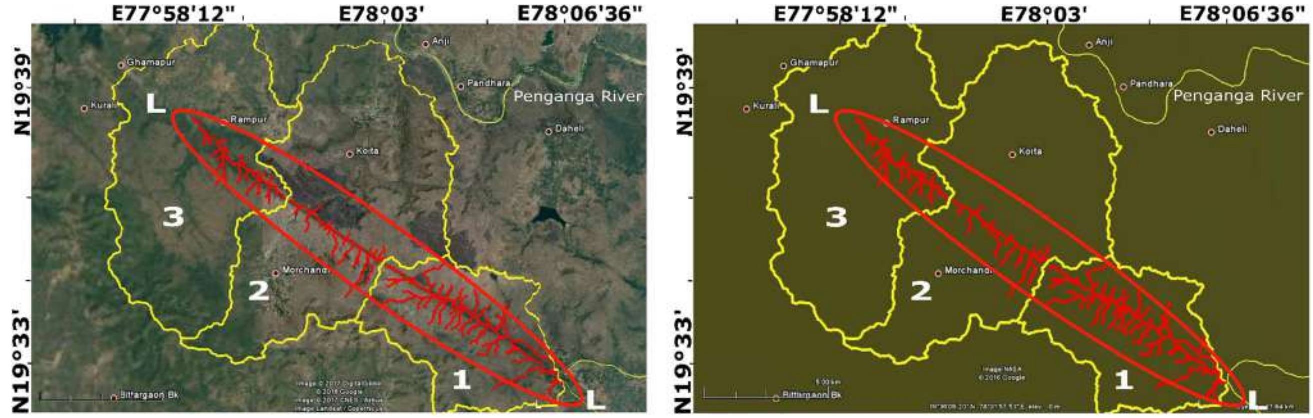

Fig. 15 **a** Un-interpreted image showing Trellis drainage pattern (circled) along the Kinwat lineament shown on Google earth image, where 1–3: sub-basins, LL: Kinwat lineament. **b** Interpreted image showing trellis drainage. The main river is Penganga river

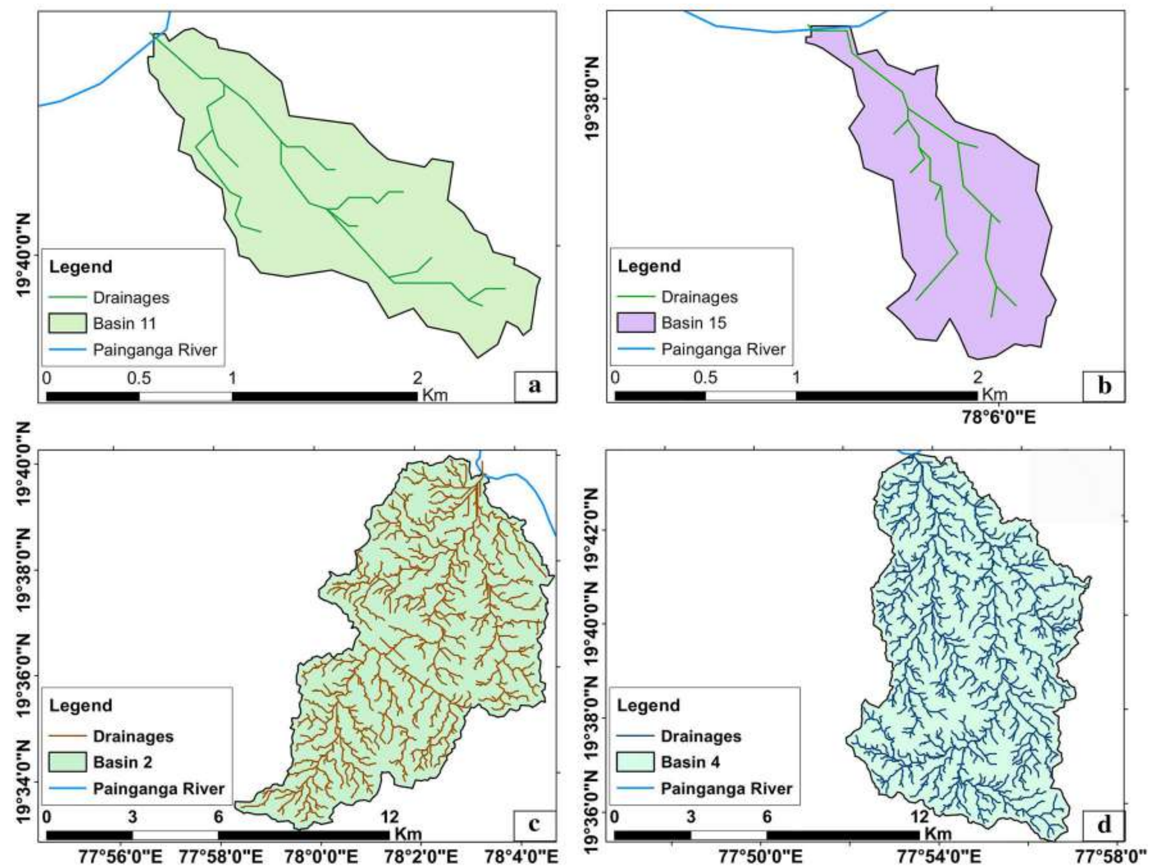

Fig. 16 Represents development of dendritic drainage pattern with different number of streams i.e. **a** Sub-basin number 11 total number of streams 11, **b** sub-basin number 15 total number of streams 10, **c** sub-basin number 2 total number of streams 538 and **d** sub-basin number 4 total number of streams 712. The sub-basins are the part of the Penganga river basin at Kinwat area in Nanded district

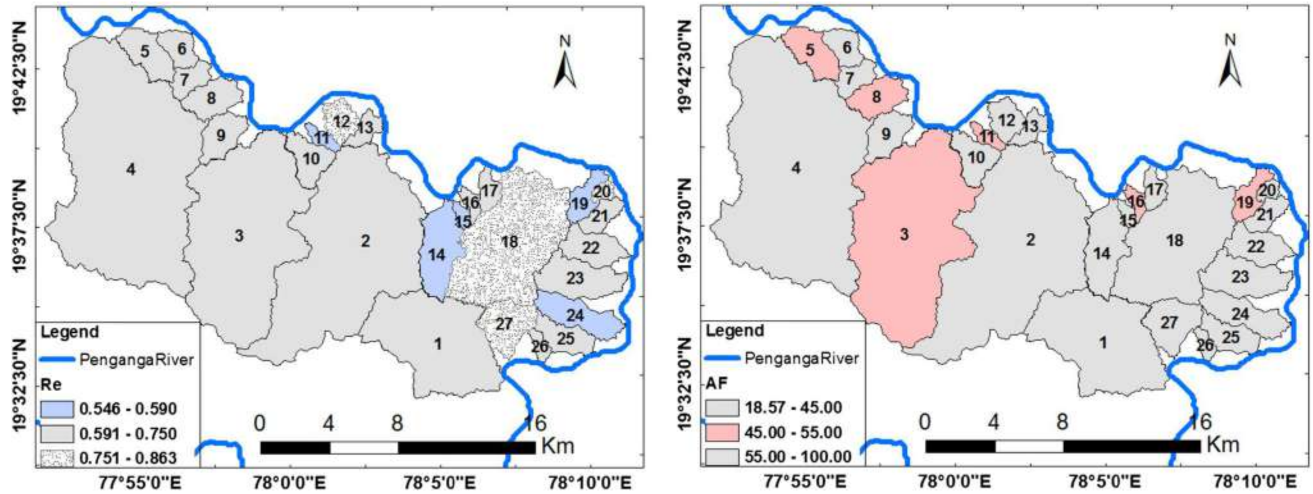

Fig. 17 Sub-basin numbers 1 to 27 showing: **a** *Re* = elongation ratio values (without unit). The colour given for *Re* 0.546–0.590 is blue colour, *Re* 0.591–0.750 grey colour, and *Re* >0.751 is marked by grey colour with dot, **b** AF = asymmetric factors (without unit). The colour given for AF 18.57–45.00 is grey colour, AF 45.00–55.00 pink colour, and AF 55.00–100.00 is marked by grey colour

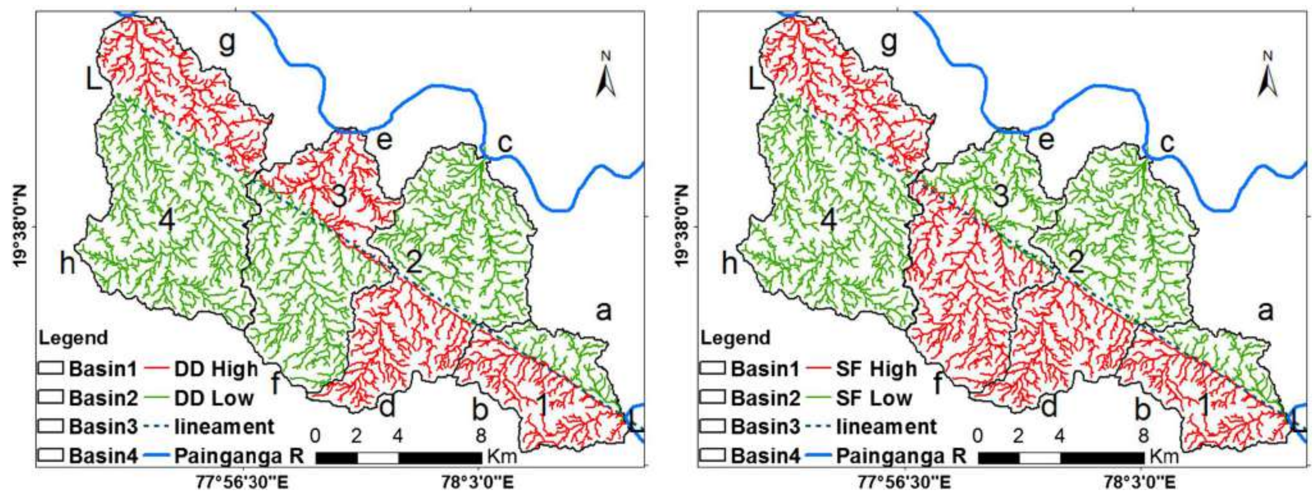

Fig. 18 Left side of the figure illustrating drainage density (DD Km/Km^2) of 4 sub-basins of Penganga river across the Kinwat lineament (L–L). Right side figure illustrates stream frequency (SF streams/Km^2) variation across the lineament. 1–4: sub-basins across Kinwat lineament (L–L). In both figures, a to g represent the part of the sub-basin showing the high or low values of DD or SF. Red colour of streams in both the figures indicate higher values of DD or SF, and green colour of streams indicates low values of DD or SF. Abbreviation R is for river

ii. Most of the study area (70%) is slightly to moderately tectonically tilted, as asymmetric factor of most of the sub-basins ranges 45–55%.

Acknowledgements R.D. Kaplay and Sumeet Chavhan thank the Director, School of Earth Sciences, S.R.T.M. University for encouragement and support. MD Babar thanks the Principal, Dnyanopasak College for her support and encouragement. S. Mukherjee was supported by internal grant and research sabbatical for the year 2017 provided by Indian Institute of Technology Bombay. Thanks go to Akash Kashyap and Narayan Bose (IIT Bombay) for support in the field and in laboratory, respectively.

References

1. Babar, Md.; Kaplay, R.D.; Mukherjee, S.; Kulkarni, P.S.: Evidences of deformation of dykes from Central Deccan Volcanic Province, Aurangabad, Maharashtra, India. In: Mukherjee S, Misra AA, Calvès G, Nemčok M (Eds) Tectonics of the Deccan Large

Igneous Province. Geol. Soc, London, Spec. Publ, **445**, 337–353 (2017).

2. Kaplay, R.D.; Babar, Md.; Mukherjee, S.; Kumar, T.V.: Morphotectonic expression of geological structures in eastern part of south east Deccan volcanic province (around Nanded, Maharashtra, India) In: Mukherjee S, Misra AA, Calvès G, Nemčok M. (Eds) Tectonics of the Deccan Large Igneous Province. Geol. Soc., London, Spec. Publ. **445**, 317–335 (2017a).
3. Kaplay, R.D.; Kumar, T.V.; Mukherjee, S.; Wesanekar, P.R.; Babar, Md; Chavhan, S.: E-W strike slip shearing of Kinwat Granitoid at South East Deccan Volcanic Province, Kinwat, Maharashtra, India. J. Earth Sys. Sci. **126**, 71 (2017)
4. Misra, A.A.; Bhattacharya, G.; Mukherjee, S.; Bose, N.: Near N-S paleo-extension in the western Deccan region, India: does it link strike-slip tectonics with India-Seychelles rifting? Int. J. Earth Sci. **103**, 1645–1680 (2014)
5. Misra, A.A.; Sinha, N.; Mukherjee, S.: Repeat ridge jumps and microcontinent separation: insights from NE Arabian Sea. Marine Petrol. Geol. **59**, 406–428 (2015)
6. Misra, A.A.; Mukherjee, S.: Atlas of Structural Geological Interpretation from Seismic Images. Wiley Blackwell (2018). ISBN: 978-1-119-15832-5
7. Misra, A.A.; Mukherjee, S.: Dyke-brittle shear relationships in the Western Deccan Strike Slip Zone around Mumbai (Maharashtra, India). In: Mukherjee, S., Misra, A.A., Calvès, G., Nemčok, M. (Eds) Tectonics of the Deccan Large Igneous Province. Geol. Soc., London, Spec. Publ. **445**, 265–295 (2017).
8. Mukherjee, S.; Misra, A.A.; Calvès, G.; Nemčok, M.: Tectonics of the Deccan Large Igneous Province: an introduction. In: Mukherjee S, Misra AA, Calvès G, Nemčok M. (Eds) Tectonics of the Deccan Large Igneous Province. Geol. Soc., London, Spec. Publ. **445**, 1–9 (2017).
9. Radhakrishnan, B.P.; Vaidyanadhan, R.: Geology of Karnataka. Second Edition. Geol Soc Ind. Bangalore. pp. 353 (1997).
10. Ramakrishanan, M.; Vaidyanandhan, R.: Geology of India. Vol 1. Geol Soc Ind. Bangalore. p. 556 (2008).
11. Condie, K.C.; Belousova, E.; Griffin, W.I.; Sircombe, K.N.: Granitoid events in space and time: constraints from igneous and detrital zircon age spectra. Gond. Res. **15**, 2128–2242 (2009)
12. Geological Survey of India: District resource map of Nanded district, Maharashtra on 1:300,000 scale with explanatory brochure (2001).
13. Banerjee, R.; Shivkumar, K.: Geochemistry and Petrogenesis of Radioactive Palaeoproterozoic Granitoids of Kinwat Crystalline Inlier, Nanded, and Yeotmal Districts. Maharashtra. J. Geol. Soc. Ind. **75**, 596–617 (2010)
14. Sangode, S.J.; Mesharm, D.C.; Kulkarni, Y.R.; Gudadhe, S.S.; Malpe, D.B.; Herlekar, M.A.: Neotectonic Response of the Godavari and Kaddam Rivers in Andhra Pradesh, India: implications to Quaternary Reactivation of Old Fracture System. J. Geol. Soc. Ind. **81**, 459–471 (2013)
15. Naganjaneyulu, K.; Dhanunjaya Naidu, G.; Someswara Rao, M.; Ravi Shankar, K.; Kishore, S.R.K.; Murthy, D.N.; Veeraswamy, K.; Harinarayana, T.: Deep crustal electromagnetic structure of central India tectonic zone and its Implications. Phys. Earth Planet. Inter. **181**, 60–68 (2010)
16. Catherine, J.K.: A preliminary assessment of internal deformation in the Indian Plate from GPS measurements. J. Asian Earth Sci. **23**, 461–465 (2004)
17. Burbank, D.W.; Anderson, R.S.: Tectonic Geomorphology. Blackwell Science. ISBN: 0 632 04386 5 (2001).
18. Keller, E.A.; Pinter, N.: Active Tectonics: Earthquakes, Uplift and Landscape, p. 337. Prentice Hall-Inc, Englewood Cliffs (1996)
19. Singh, T.: Tectonic implications of geomorphic characterization of watersheds using spatial correlation: mohand Ridge, NW Himalaya, India. Zeitschrift für Geomorphologie **54**, 489–501 (2008)
20. Singh, T.: Hypsometric analysis of watersheds developed on actively deforming Mohand anticlinal ridge, NW Himalaya. Geocarto. Int. **23**, 417–427 (2008)
21. Passchier, C.W.; Trouw, R.A.J.: Microtectonics, 2nd edn. Springer, Berlin (2005)
22. Mukherjee, S: Geodynamics, deformation and mathematical analysis of metamorphic belts of the NW Himalaya. Ph.D. thesis. Indian Institute of Technology Roorkee (2007).
23. Mukherjee, S.: Structures in Meso- and Micro-scales in the Sutlej section of the Higher Himalayan Shear Zone, Indian Himalaya. e-Terra **7**, 1–27 (2010)
24. Mukherjee, S.: Microstructures of the Zanskar shear zone. Earth Sci. Ind. **3**, 9–27 (2010)
25. Mukherjee, S.: Flanking microstructures from the Zanskar Shear Zone, NW Indian himalaya. YES Bull. **1**, 21–29 (2011)
26. Mukherjee, S.: Mineral Fish: their morphological classification, usefulness as shear sense indicators and genesis. Int. J. Earth Sci. **100**, 1303–1314 (2011)
27. Mukherjee, S.: Tectonic implications and morphology of trapezoidal mica grains from the Sutlej section of the Higher Himalayan Shear Zone, Indian Himalaya. The J. Geol. **120**, 575–590 (2012)
28. Mukherjee, S.: Simple shear is not so simple! Kinematics and shear senses in Newtonian viscous simple shear zones. Geol. Mag. **149**, 819–826 (2012)
29. Mukherjee, S.: Higher Himalaya in the Bhagirathi section (NW Himalaya, India): its structures, backthrusts and extrusion mechanism by both channel flow and critical taper mechanisms. Int. J. Earth Sci. **102**, 1851–1870 (2013)
30. Mukherjee, S.: Deformation Microstructures in Rocks. Springer Geochemistry/Mineralogy. Berlin. pp. 1–111 (2013b).
31. Mukherjee, S.: Mica inclusions inside host mica grains from the sutlej section of the higher himalayan crystallines, India- morphology and constrains in genesis. Acta Geol. Sinica **88**, 1729–1741 (2014)
32. Mukherjee, S.: Review of flanking structures in meso- and micro-scales. Geol. Mag. **151**, 957–974 (2014)
33. Mukherjee, S.: Kinematics of ‘top -to-down’ simple shear in a Newtonian Rheology. The J. Ind. Geophys. Union **18**, 245–248 (2014)
34. Mukherjee, S.: Review on symmetric structures in ductile shear zones. Int. J. Earth Sci. **106**, 1453–1468 (2017)
35. Mukherjee, S.; Koyi, H.A.: Flanking microstructures. Geol. Mag. **146**, 517–526 (2009)
36. Mukherjee, S.; Koyi, H.A.: Higher Himalayan Shear Zone, Zanskar section- microstructural studies & extrusion mechanism by a combination of simple shear & channel flow. Int. J. Earth Sci. **99**, 1083–1110 (2010)
37. Mukherjee, S.; Koyi, H.A.: Higher Himalayan Shear Zone, Sutlej Section- Structural Geology & Extrusion Mechanism by Various Combinations of Simple Shear, Pure Shear & Channel Flow in Shifting Modes. Int. J. Earth Sci. **99**, 1267–1303 (2010)
38. Dasgupta, S.; Mukherjee, S.: 2017) Brittle shear tectonics in a narrow continental rift: asymmetric non-volcanic Barmer basin (Rajasthan, India. The J Geol. **125**, 561–591 (2017)
39. Deng, Q.; Wu, D.; Zhang, P.; Chen, S.: Structure and deformational character of strike-slip fault zones. Pure. Appl. Geophys. **124**, 203–223 (1986)
40. Cuong, N.Q.; Zuchiewicz, W.A.: Morphotectonic properties of the Lo River Fault near Tam Dao in North Vietnam. J. Nat. Hazards Earth Syst. Sci. **1**, 15–22 (2001)

41. Johnson, K.M.; Hsu, Y.-J.; Segall, P.; Yu, S.B.: Fault geometry and slip distribution of the 1999 Chi-Chi, Taiwan earthquake imaged from inversion of GPS data. Geophys. Res. Lett. **28**, 2285–2288 (2001)

42. Hare, P.H.; Gardner, T.W.: Geomorphic indicators of vertical neotectonism along converging plate margins, Nicoya Peninsula, Costa Rica. In: Morisawa, M., Hack, J.T. (eds.) Tectonic Geomorphology, pp. 75–104. Allen and Unwin, Boston (1985)